401 N. Lindbergh Blvd.
St. Louis, MO 63141
Tel.: 314.993.1700, #546
Toll Free: 800.424.2841, #546
Fax: 800.708.1364
Cell: 314.283.1983
Send via email to: jbode@aaortho.org and cyoung@aaortho.org

AAO Foundation Final Report Form
(a/o 6/30/2020)

In an attempt to make things a little easier for the reviewer who will read this report, please consider these two questions before this is sent for review:

- *Is this an example of your very best work, in that it provides sufficient explanation and justification, and is something otherwise worthy of publication? (We do publish the Final Report on our website, so this does need to be complete and polished.)*
- *Does this Final Report provide the level of detail, etc. that you would expect, if you were the reviewer?*

Please prepare a report that addresses the following:

Type of Award: Orthodontic Faculty Development Fellowship Award

Name(s) of Principal Investigator(s): Marilia Yatabe

Institution: University of Michigan

Title of Project: Biomaterials for regeneration of palatal defects

Period of AAOF Support: 07-01-20 to 06-30-21 (No cost extension until 06-30-2022)

Amount of Funding: $ 20,000.00

Summary/Abstract

Introduction: Current surgical techniques to repair the palatal defect in patients with cleft palate often results in adverse consequences to the maxillary growth and development. To improve the oral rehabilitation while minimizing the side effects, different biomaterials have been studies in animal models. Histological analysis revealed fibrous tissue, blood capillary and small gland-like constructs, collagen fibers, new bone tissue, keratinocytes, monocytes, and macrophages[24,25,26] While the current tested biomaterials have their advantages and disadvantages, the ideal biomaterial would be biocompatible, absorbable, have mechanical stability, provide a platform for bone cells to proliferate, be easy to sterilize, manufacture and handle in the operating room, and have sufficient porosity to accommodate osteoblasts, support cell proliferation and differentiation and enhance bone tissue formation[11]. Therefore, the purposes of this study were to (1) verify if the 3D printed Acrylated Poly-Glycerol-Dodecanedioate (APGD), a biodegradable, biocompatible shape memory polymer, is biocompatible to the oral cavity, (2) determine if APGD is a viable scaffold for cellular proliferation, (3) investigate histological methods to determine cellular activity during wound healing, and (4) three-dimensionally assess changes in the maxillary alveolar bone and/or teeth.

Material and Methods: This preliminary experiment has been approved by the IACUC at the University of Michigan (PRO00008013). The sample comprised 16 male rats, 16 weeks of age, divided into 2 groups: 8 rats in the experimental group (APGD) and 8 rats in the control group (C), which were subdivided by euthanasia timing: half of each sample was euthanized 4 weeks after procedure, and the other half, 12 weeks after the procedure. All animals were maintained in the animal facility at the University of Michigan with 2 animals per cage, water and rodent soft chow *ad libitum*. Surgical protocol: (1) Proper Anesthesia and analgesia were performed. (2) A critical size defect of 1.5mm diameter was made in the middle of the hard palate. (3) For the experimental group, a 3D printed APGD was placed in the defect, while in the control group, the defect was left open. Survival rate and pain were monitored daily. Four and 12 weeks later, animals were euthanized by carbon dioxide overdose followed by bilateral pneumothorax. The maxilla was excised for micro-CT and histological analysis. Micro-CT images were taken at four different timepoints: pre-surgery (T0), immediately post-surgery (T1), 4-weeks post-euthanasia (T2), and 12-weeks post-euthanasia (T3). Each scan was oriented, cropped, and registered to the specific region of interest (maxilla) using 3D-Slicer, and anatomical landmark points were pre-labeled using ITK-SNAP. The Q3DC tool in 3D-Slicer was used to place points on the pre-labeled landmarks and to record maxillary three-dimensional measurements along with molar angulation. The different timepoint scans of each rat were then superimposed via voxel-based registration in 3D-Slicer for further visualization of these changes. Mean, standard deviation, and differences between timepoints within each group were computed. Independent t-tests were

calculated between groups. For histological analysis, after excision, specimens were decalcified, and processed for cryosectioning. The sections were stained with Hematoxylin & Eosin (H&E), Masson's trichrome, Tartrate-resistant acid phosphatase (TRAP), Beta-Catenin and Ki67 Immunohistochemistry (IHC). Analysis: Micro-CT scans were performed by one operator using the same scanner (Skyscan 1176, Bruker µCT, Kontich, Belgium) and with the following protocol: all animals scanned in water, with 16µm (in-vivo) or 9µm (ex-vivo) isotropic voxel, 1mm Aluminum filter, 0.3º rotation step, 2 frame averaging, 65 kV source voltage and 385 µA source current. Immediately after euthanasia, the maxillary specimen was excised and placed in fixation to be later processed for histological analysis using the following staining: Hematoxylin and Eosin, Masson's Trichrome, TRAP, Beta-Catenin and Ki67.

Results: Three-dimensional assessment showed that from T0-T1 there were no notable transverse changes at the levels of the roots, crowns, and alveolar crests. Overall transverse changes between T1-T2 were similar between groups, with greater changes observed between T1-T3. The molar buccal-lingual inclinations were similar between the control and experimental groups at all time points. Fibrous connective tissue was noted in both groups and inflammatory cell activity was increased qualitatively in the APGD sample compared to the control sample at both time points. The four-week APGD group had a noticeable osteoclastic response to the scaffold material and a disrupted oral epithelial layer. The APGD scaffold was not present in the twelve-week sample.

Conclusions: APGD did not have a major overall impact on the hard tissue of the rat maxilla when compared to the control group. Skeletal expansion and dental buccal-lingual inclinations changes were observed, albeit non-significant, in both control and experimental groups, suggesting that other factors aside from APGD may be leading to these effects. Histologically, there was an increased inflammatory reaction and bone resorptive response from the 3D printed APGD scaffold and wound healing in the rat model suggests an increased inflammatory reaction and bone resorptive response when compared to the control with no scaffold.

Detailed results and inferences:

Table 1. Mean and standard deviation - (SD) - of the three-dimensional, antero-posterior, transversal, and vertical changes between T1-T2 of each point in each group.

	T1-T2 Control	T1-T2 APGD	T1-T2 Control	T1-T2 APGD	T1-T2 Control	T1-T2 APGD	T1-T2 Control	T1-T2 APGD
	R-L Component		A-P Component		S-I Component		3D Distance	
Rt-1 - Rt-1	0.10	0.01 (0.00)	-0.05	0.04 (0.05)	0.01	0.02 (0.07)	0.11	0.08 (0.01)
Rt-2 - Rt-2	0.17	0.08 (0.06)	-0.13	0.16 (0.13)	0.11	0.08 (0.10)	0.24	0.20 (0.17)
Rt-3 - Rt-3	0.01	0.02 (0.03)	-0.07	0.04 (0.10)	0.10	0.03 (0.11)	0.13	0.12 (0.01)
Rt-4 - Rt-4	0.07	0.02 (0.02)	-0.16	0.03 (0.03)	0.02	0.07 (0.10)	0.17	0.10 (0.08)
Rt-5 - Rt-5	0.08	0.05 (0.13)	-0.17	0.04 (0.02)	0.14	0.04 (0.05)	0.24	0.12 (0.05)
Rt-6 - Rt-6	-0.01	0.01 (0.08)	-0.10	-0.09 (0.04)	0.10	0.06 (0.07)	0.14	0.12 (0.07)
Rt-7 - Rt-7	-0.07	0.07 (0.22)	-0.17	0.12 (0.14)	-0.02	0.01 (0.04)	0.19	0.20 (0.16)
Rt-8 - Rt-8	0.08	0.06 (0.05)	-0.06	-0.02 (0.04)	0.00	0.09 (0.02)	0.10	0.12 (0.01)
Rt-9 - Rt-9	0.10	0.05 (0.17)	-0.11	0.06 (0.05)	-0.02	0.04 (0.01)	0.15	0.14 (0.08)
Rt-10 - Rt-10	0.09	0.10 (0.13)	-0.12	-0.03 (0.08)	0.01	0.05 (0.07)	0.15	0.15 (0.09)
Rt-11 - Rt-11	0.05	0.08 (0.19)	-0.07	-0.02 (0.03)	-0.05	0.05 (0.00)	0.09	0.15 (0.11)
Rt-12 - Rt-12	-0.01	0.07 (0.03)	-0.03	0.06 (0.02)	0.08	-0.02 (0.11)	0.09	0.12 (0.05)
Rt-13 - Rt-13	-0.21	-0.05 (0.21)	-0.28	0.08 (0.01)	0.14	0.04 (0.19)	0.38	0.21 (0.09)
Rt-14 - Rt-14	0.00	0.08 (0.02)	0.03	0.10 (0.04)	0.14	0.05 (0.15)	0.14	0.17 (0.06)
Rt-15 - Rt-15	-0.13	-0.04 (0.11)	0.02	0.13 (0.13)	0.19	0.08 (0.15)	0.23	0.19 (0.18)
Rt-16 - Rt-16	0.01	-0.05 (0.07)	-0.07	0.03 (0.05)	0.12	0.01 (0.10)	0.14	0.10 (0.06)
Rt-17 - Rt-17	0.13	0.02 (0.05)	-0.06	0.02 (0.09)	0.27	0.09 (0.14)	0.30	0.14 (0.10)
Rt-18 - Rt-18	0.03	-0.06 (0.03)	-0.06	0.07 (0.05)	0.09	0.04 (0.14)	0.11	0.15 (0.02)
Rt-19 - Rt-19	-0.01	-0.06 (0.11)	0.04	0.01 (0.01)	0.09	0.07 (0.14)	0.10	0.12 (0.13)
Rt-20 - Rt-20	0.01	-0.06 (0.06)	-0.10	0.05 (0.00)	0.04	0.06 (0.09)	0.11	0.11 (0.08)
Rt-21 - Rt-21	-0.12	-0.04 (0.08)	-0.12	0.01 (0.02)	0.09	0.07 (0.05)	0.19	0.09 (0.06)
Rt-22 - Rt-22	0.10	-0.02 (0.12)	-0.05	0.02 (0.10)	0.05	0.10 (0.11)	0.12	0.16 (0.07)
AC-1 - AC-1	0.01	0.04 (0.06)	-0.10	-0.08 (0.04)	-0.12	-0.12 (0.19)	0.16	0.19 (0.13)
AC-2 - AC-2	0.09	0.05 (0.00)	-0.10	-0.02 (0.12)	-0.16	-0.12 (0.10)	0.21	0.16 (0.05)
AC-3 - AC-3	0.08	0.09 (0.02)	-0.12	-0.01 (0.10)	-0.21	-0.10 (0.06)	0.26	0.16 (0.04)
AC-4 - AC-4	0.15	-0.06 (0.41)	-0.07	-0.01 (0.07)	-0.15	0.13 (0.35)	0.23	0.39 (0.18)
AC-5 - AC-5	-0.03	0.00 (0.02)	-0.19	-0.07 (0.08)	-0.07	-0.44 (0.36)	0.20	0.44 (0.37)
AC-6 - AC-6	-0.05	-0.15 (0.04)	0.01	-0.11 (0.05)	-0.09	-0.09 (0.11)	0.11	0.22 (0.00)
AC-7 - AC-7	-0.03	-0.12 (0.08)	0.01	-0.08 (0.07)	-0.15	-0.11 (0.07)	0.15	0.19 (0.06)
AC-8 - AC-8	-0.09	-0.03 (0.08)	-0.03	0.05 (0.04)	-0.14	0.02 (0.17)	0.17	0.15 (0.02)
Cr-1 - Cr-1	0.13	0.03 (0.01)	-0.06	-0.04 (0.09)	0.01	0.05 (0.15)	0.14	0.14 (0.03)
Cr-2 - Cr-2	0.03	0.03 (0.04)	-0.13	-0.03 (0.07)	-0.07	0.05 (0.10)	0.15	0.11 (0.05)
Cr-3 - Cr-3	0.00	0.06 (0.12)	-0.12	0.06 (0.11)	-0.13	0.04 (0.04)	0.17	0.14 (0.09)
Cr-4 - Cr-4	0.10	0.02 (0.03)	-0.01	0.15 (0.01)	0.11	-0.02 (0.14)	0.14	0.19 (0.01)
Cr-5 - Cr-5	-0.01	-0.09 (0.02)	-0.09	-0.03 (0.03)	0.07	-0.01 (0.08)	0.11	0.11 (0.01)
Cr-6 - Cr-6	-0.03	-0.02 (0.00)	0.03	0.03 (0.12)	-0.06	0.01 (0.06)	0.07	0.10 (0.03)

Table 2 – Transverse dimensions for each group and time point, along with a statistical comparison between C and APGD groups at T2 and T3.

	T0 Control	T1 Control	T1 APGD	Difference	T2 Control	T2 APGD	Difference	*p*	T3 Control	T3 APGD	Difference	*p*
Rt-1 - Rt-12	8.16 (0.27)	8.37	8.16 (0.16)	0.22	8.00 (0.69)	8.20 (0.08)	-0.20	0.76	7.75 (0.52)	8.19 (0.25)	-0.45	0.28
Rt-2 - Rt-13	4.58 (0.04)	4.50	4.59 (0.18)	-0.09	4.80 (0.10)	4.74 (0.14)	0.06	0.66	4.63 (0.09)	4.71 (0.40)	-0.09	0.75
Rt-3 - Rt-14	7.52 (0.54)	8.00	7.50 (0.15)	0.50	7.59 (0.58)	7.45 (0.13)	0.14	0.79	7.19 (0.27)	7.59 (0.24)	-0.40	0.13
Rt-4 - Rt-15	4.92 (0.21)	5.10	4.94 (0.11)	0.17	5.20 (0.14)	4.95 (0.00)	0.25	0.23	4.94 (0.27)	5.40 (0.07)	-0.46	0.09
Rt-5 - Rt-16	7.53 (0.49)	7.84	7.45 (0.18)	0.39	7.50 (0.60)	7.61 (0.28)	-0.11	0.85	7.33 (0.32)	7.53 (0.37)	-0.20	0.53
Rt-6 - Rt-17	4.51 (0.16)	4.61	4.75 (0.19)	-0.14	4.58 (0.14)	4.84 (0.18)	-0.26	0.25	4.36 (0.26)	5.06 (0.10)	-0.70	0.03
Rt-7 - Rt-18	6.57 (0.50)	7.07	6.62 (0.20)	0.45	6.64 (0.46)	6.87 (0.45)	-0.23	0.66	6.55 (0.35)	6.75 (0.05)	-0.20	0.43
Rt-8 - Rt-19	4.68 (0.20)	4.93	4.70 (0.21)	0.23	4.79 (0.31)	4.88 (0.23)	-0.09	0.79	4.76 (0.21)	5.00 (0.25)	-0.24	0.39
Rt-9 - Rt-20	6.70 (0.36)	7.03	6.90 (0.40)	0.12	7.01 (0.14)	7.24 (0.49)	-0.23	0.63	7.05 (0.09)	7.17 (0.36)	-0.12	0.62
Rt-10 - Rt-21	4.55 (0.42)	4.95	4.81 (0.18)	0.14	5.11 (0.07)	5.07 (0.29)	0.04	0.88	4.96 (0.24)	5.04 (0.19)	-0.08	0.67
Rt-11 - Rt-22	5.33 (0.00)	5.36	5.32 (0.11)	0.04	5.29 (0.02)	5.39 (0.28)	-0.10	0.69	5.36 (0.01)	5.43 (0.16)	-0.06	0.57
MP-R1M - MP-L1M	6.30 (0.25)	6.49	6.30 (0.09)	0.20	6.40 (0.38)	6.34 (0.02)	0.06	0.85	6.12 (0.26)	6.53 (0.12)	-0.40	0.11
MP-R2M - MP-L2M	5.82 (0.34)	6.11	5.88 (0.16)	0.23	5.88 (0.31)	6.05 (0.29)	-0.17	0.62	5.75 (0.28)	6.13 (0.12)	-0.38	0.13
MP-R3M - MP-L3M	5.48 (0.20)	5.67	5.59 (0.17)	0.09	5.67 (0.07)	5.77 (0.34)	-0.10	0.75	5.73 (0.00)	5.77 (0.17)	-0.03	0.76
AC-1 - AC-5	8.11 (0.28)	8.41	8.20 (0.09)	0.21	8.30 (0.24)	8.19 (0.14)	0.12	0.62	8.07 (0.28)	8.28 (0.16)	-0.21	0.34
AC-2 - AC-6	8.80 (0.24)	8.95	8.86 (0.12)	0.09	8.86 (0.34)	9.00 (0.06)	-0.14	0.68	8.72 (0.14)	9.01 (0.19)	-0.29	0.11
AC-3 - AC-7	8.81 (0.20)	8.93	8.95 (0.09)	-0.02	8.94 (0.17)	9.18 (0.22)	-0.24	0.35	9.07 (0.10)	9.30 (0.05)	-0.23	0.04
AC-4 - AC-8	8.07 (0.28)	8.23	8.04 (0.20)	0.19	8.30 (0.26)	8.04 (0.55)	0.26	0.62	8.31 (0.14)	8.65 (0.05)	-0.33	0.04
Cr-1 - Cr-4	6.96 (0.26)	7.14	7.07 (0.16)	0.07	6.91 (0.38)	7.14 (0.01)	-0.23	0.55	6.85 (0.23)	7.06 (0.23)	-0.21	0.32
Cr-2 - Cr-5	6.99 (0.08)	7.10	7.20 (0.12)	-0.10	7.07 (0.10)	7.33 (0.20)	-0.26	0.29	7.39 (0.07)	7.43 (0.25)	-0.05	0.79
Cr-3 - Cr-6	6.73 (0.15)	6.99	6.97 (0.18)	0.02	6.97 (0.08)	7.15 (0.41)	-0.18	0.64	7.20 (0.12)	7.38 (0.23)	-0.18	0.33

Table 3 – Angles between the right and left molars at each time point for all the samples with at least two different time points to compare.

	1 RM / LM				2 RM / LM				3 RM / LM			
	T0	T1	T2	T3	T0	T1	T2	T3	T0	T1	T2	T3
Average	19.53	22.74	21.13	18.97	37.67	40.71	38.25	43.01	44.19	49.07	48.42	52.40
SD	0.64	3.07	6.16	0.54	6.76	4.75	4.91	4.11	1.86	5.86	5.49	5.69

Table 4 – Angular changes for each tooth across all time points. Positive values indicate a clockwise rotation, and negative values indicate a counterclockwise rotation.

	1 RM			1 LM			2 RM			2 LM			3 RM			3 LM		
	T0-T1	T1-T2	T1-T3	T0-T1	T1-T2	T1-T3	T0-T1	T1-T2	T1-T3	T0-T1	T1-T2	T1-T3	T0-T1	T1-T2	T1-T3	T0-T1	T1-T2	T1-T3
Average	-0.01	0.24	-1.83	0.88	2.07	1.54	-0.11	-0.63	-1.47	0.14	-0.86	-0.70	1.65	-1.58	1.63	-2.28	0.87	-1.75
SD		0.72	0.28		2.96	2.81		2.43	2.43		1.34	0.82		2.46	4.55		2.56	1.36

Figure 1 – Example of T3 (Blue) superimposed to T1 (White). Note the expanded maxilla and 2nd and 3rd molars in the APGD Group.

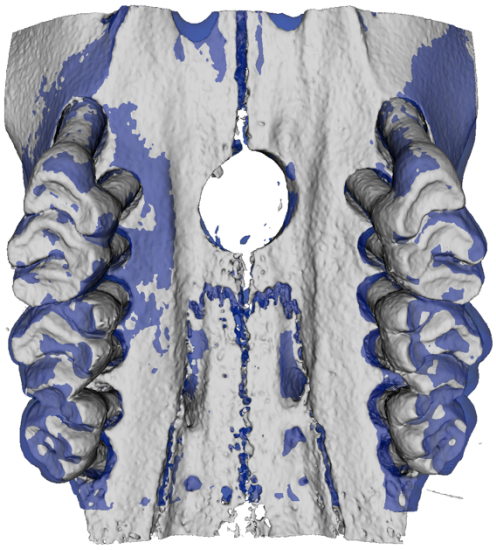

Inferior

Superior

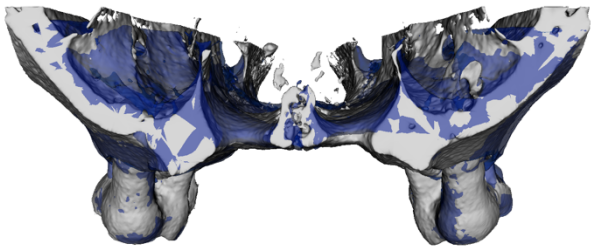

Anterior

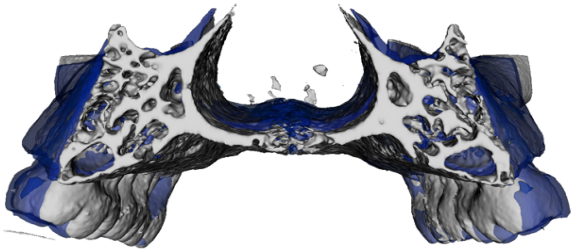

Posterior

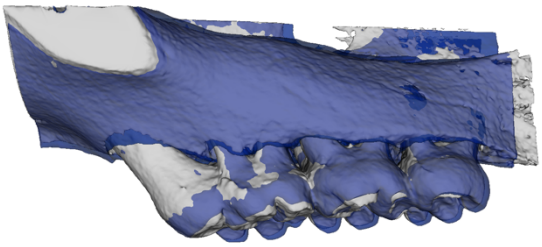

Right side

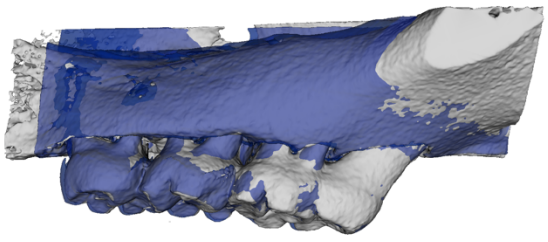

Left side

Figure 2 – Example of T2 (Red) superimposed to T1 (White). Note the expanded maxilla and 2nd and 3rd molars in the Control Group.

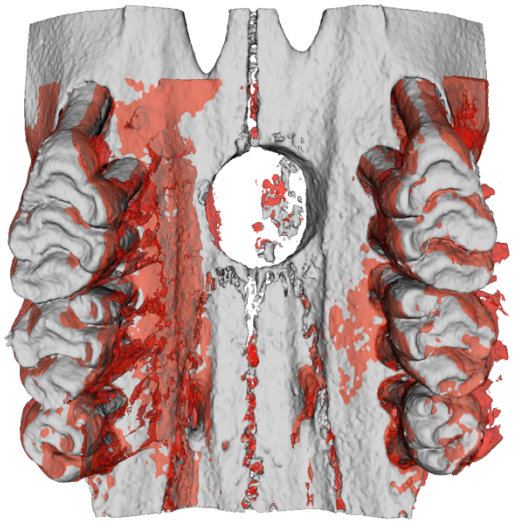

Inferior

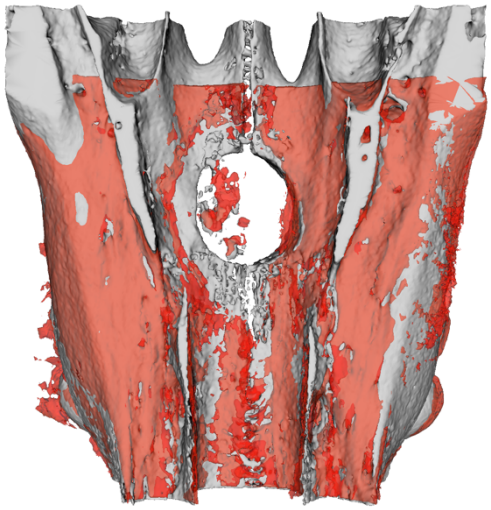

Superior

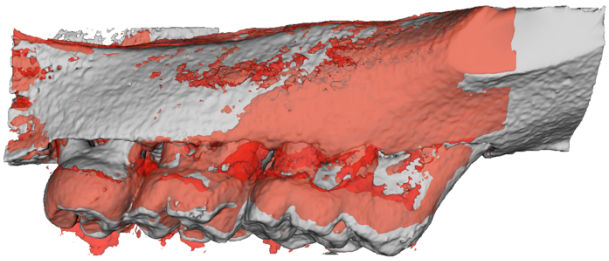

Right side

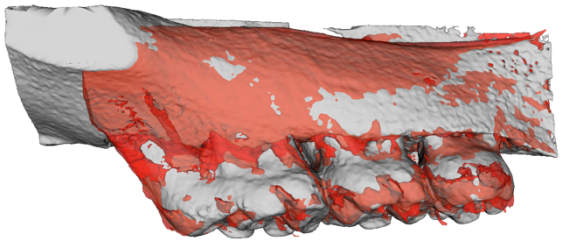

Left side

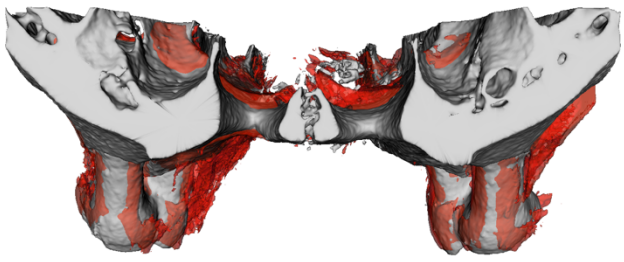

Anterior

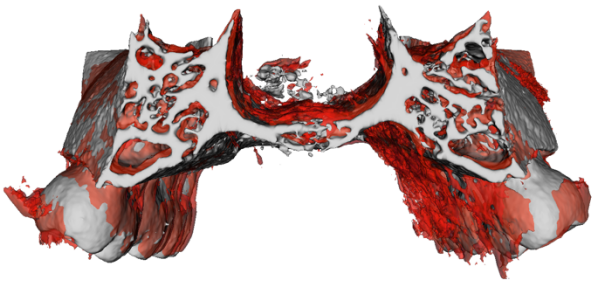

Posterior

Table 5 – Summary of the histological findings.

Stain	Purpose	Time	Control	APGD
Hematoxylin & Eosin (H&E)	-microanatomy of organs/tissues -inflammation -quality of soft tissue healing	4w	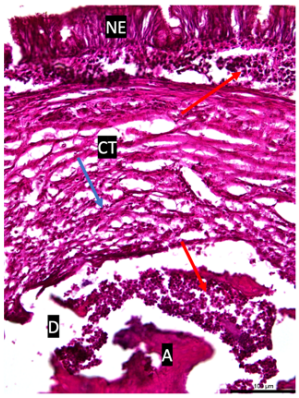 Artifacts (A); Nasal epithelium (NE); Connective Tissue (CT); Defect (D). Red arrow - lymphocyte infiltration NE, granulated CT and D. Blue arrow - Fibroblasts throughout the CT.	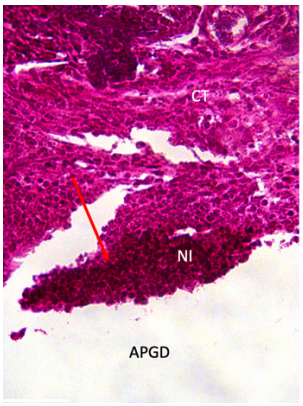 Nasal interface (NI). Red arrow indicates lymphocytes at NI.
		12w	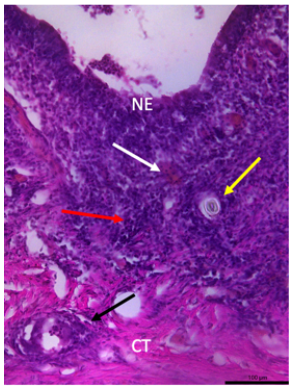 Nasal epithelium (NE); Connective tissue (CT). Red arrow – Lymphocytes. White arrow – Red blood cells. Yellow arrow – Foreign object. Black arrow - Multinucleated giant cell, characterized as large cells with numerous small dark, round nuclei.	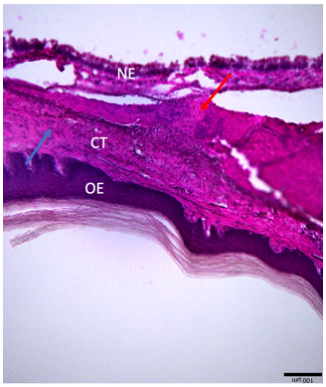 Connective tissue (CT); nasal (NE) and oral epithelia (OE). Red arrow – Lymphocytes. Blue arrow - Fibroblasts.

Masson’ s Trichrome	-connective tissue fibers -bone vs. soft tissue healing	4w	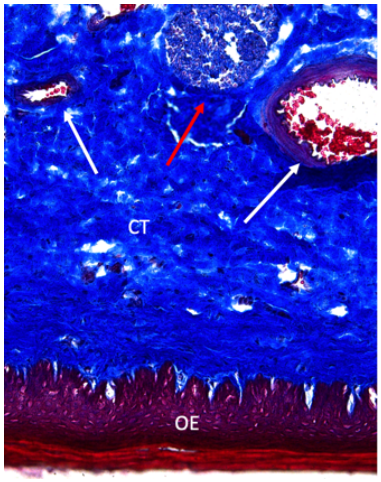 Oral epithelial (OE). Connective tissue (CT) White arrow - Blood vessels Red arrow - Salivary gland tissue.	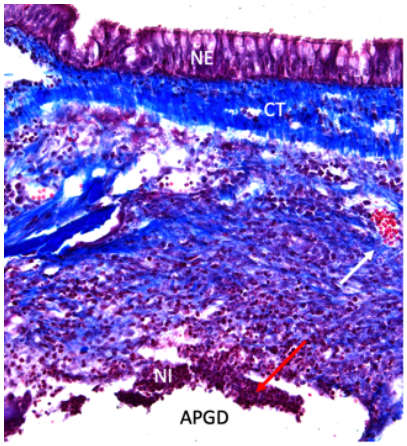 Nasal interface (NI); Nasal epithelium (NE); Connective tissue (CT). Red arrow – Lymphocytes.
		12w	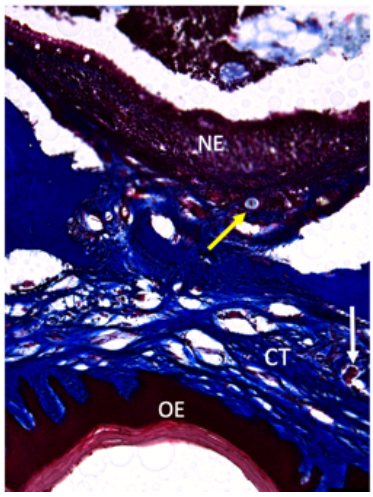 Connective tissue (CT). Nasal (NE) and oral epithelium (OE) White arrow – Blood vessels. Yellow arrow – Foreign body object.	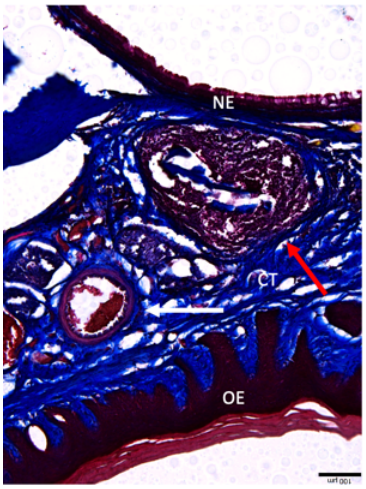 Nasal (NE) and oral (OE) epithelium. Connective tissue (CT). White arrow – Red blood vessels Red arrow – Lymphocytes.

<table>
<tr><td rowspan="2">Tartrate-resistant acid phosphatase (TRAP)</td><td rowspan="2">-osteoclasts; macrophages; dendritic cells
-identification of bone activity</td><td>4w</td><td> 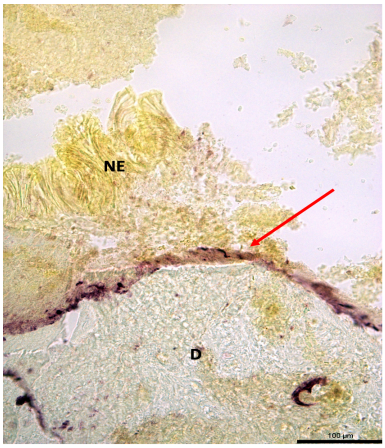

Nasal epithelium (NE).
Defect (D)
Red arrow - Osteoclast activity.</td><td> 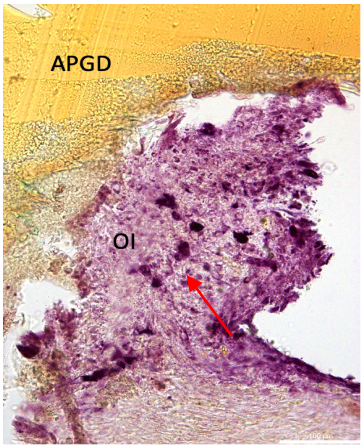

Oral interface (OI).
Red arrow – osteoclasts.</td></tr>
<tr><td>12w</td><td> 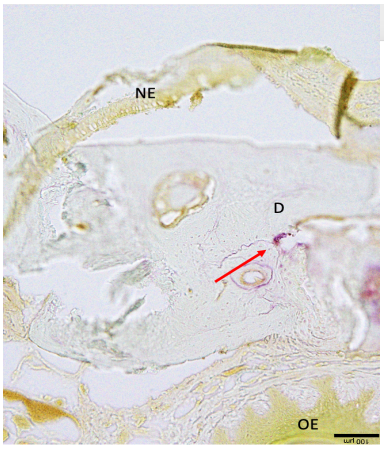

Nasal (NE) and oral (OE) epithelium.
Defect (D)
Red arrow – osteoclastic activity.</td><td> 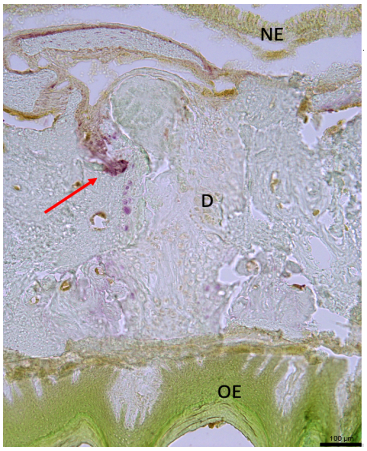

Nasal (NE) and oral (OE) epithelium.
Defect (D)
Red arrow – osteoclastic activity.</td></tr>
</table>

Beta-catenin Immunohistochemistry (IHC)	Protein beta-catenin -identification of epithelial layers during wound healing	4w	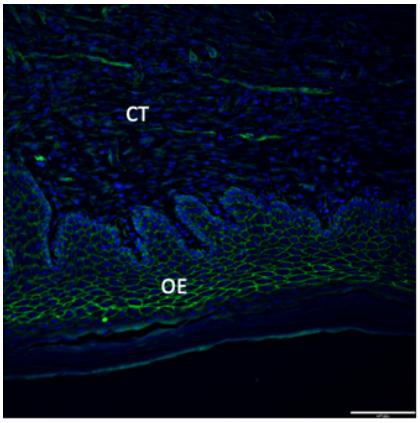 Oral epithelium (OE). Connective tissue (CT).	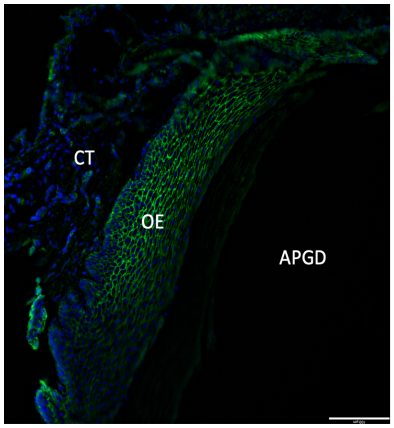 Oral epithelium (OE). Connective tissue (CT).
		12w	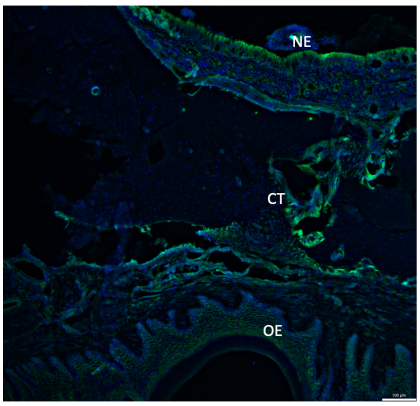 Nasal (NE) and stratified squamous oral (OE) epithelial layers.	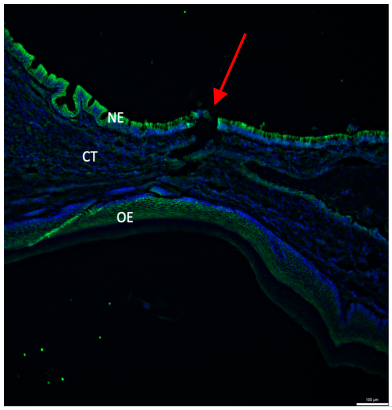 Nasal (NE) and oral (OE) epithelial. Red arrow - Break in pseudostratified columnar ciliated NE.

Ki67 Immunohistochemistry (IHC)	-Ki67 -identification of actively proliferating cells during wound healing	4w	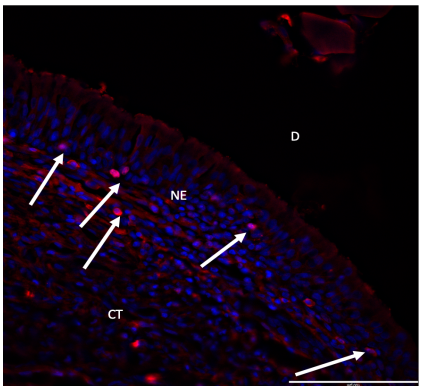 Nasal epithelium (NE). White arrows - proliferative activity at the basal layer of the NE.	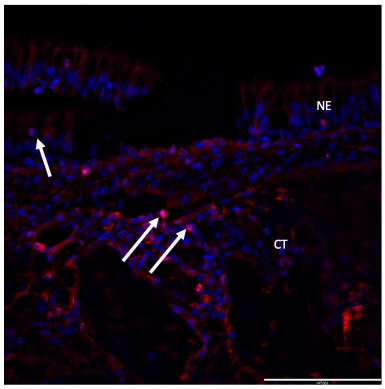 Nasal epithelium (NE). White arrows - proliferating cells at the basal layer of the NE.
		12w	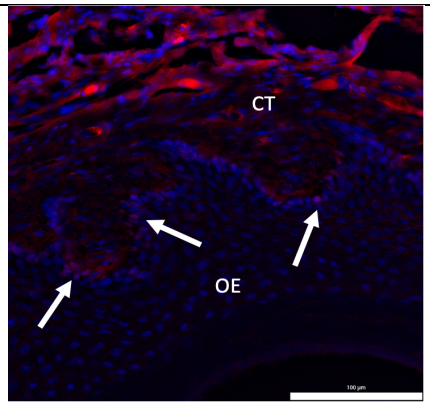 Oral epithelium (OE). Connective tissue (CT). White arrows - little proliferation at the base of the OE.	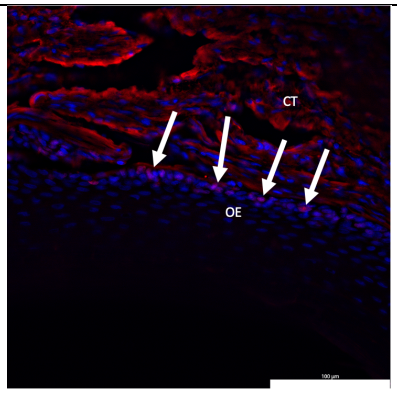 Oral epithelium (OE). Connective tissue (CT). White arrows - little proliferation at the base of the OE.

Respond to the following questions:

1. Were the original, specific aims of the proposal realized?

   Yes, the objectives of the proposed research have been achieved. We have adjusted the methodology analysis to optimize the results' assessment of the proposed study.

2. Were the results published?

   Manuscripts regarding the histological and three-dimensional changes found in the defected palate after the use of a biomaterial are in preparation. AAOF support will be acknowledged.

3. Have the results of this proposal been presented?

   We plan to present the outcomes of this study in research meetings, even though they were not as favorable as hypothesized. AAOF support will be acknowledged.

4. To what extent have you used, or how do you intend to use, AAOF funding to further your career?

   The AAOF funding was fundamental to financially support the preliminary data of a promising research as well as my salary. As a junior faculty, it is important and encouraging to have AAOF recognizing that our research has potential to improve the care for patients with craniofacial anomalies. The AAOF funding has strengthened my CV as well as motivated to continue to aim high on my career and research goals.